ISSN 1330-3651 (Print), ISSN 1848-6339 (Online) https://doi.org/10.17559/TV-20220806130349
Original scientific paper

Smooth Regulation of DC Voltage in VSC-MTDC Systems Based on Optimal Adaptive Droop Control

Ping HE*, Xiaowei ZHANG, Congshan LI, Lei YUN, Hua YANG, Yabang YAN

Abstract: DC voltage stability and power balance are the key conditions for stable operation of DC transmission systems. The droop control does not depend on inter-station communication and has the advantage of multi-station cooperative unbalanced power dissipation, which has been widely used in the voltage source converter based multi-terminal direct current (VSC-MTDC) system. However, its control will cause DC voltage deviation, and there are a series of problems such as unstable system control and overload operation of the VSC-station due to improper setting of droop coefficient. In this paper, the infeasibility of DC voltage error-free correction under droop control mode is theoretically analyzed, and a VSC-MTDC cooperative optimization droop control strategy with DC voltage "quasi-error-free" adjustment ability is proposed. The strategy adjusts the droop coefficient in real-time by monitoring the DC voltage deviation and the power margin of the VSC-station to solve the problem of voltage deviation caused by unbalanced power consumption. At the same time, an additional DC voltage stabilizer is designed to automatically adjust the power reference value and restore the DC voltage. Finally, a five-terminal VSC-MTDC system is built under PSCAD/EMTDC to verify the feasibility of the proposed strategy.

Keywords: DC voltage deviation; droop control; power margin; VSC-MTDC

1 INTRODUCTION

With the continuous adjustment of energy structure, the penetration rate of large-capacity power electronic devices in the power grid has gradually increased, and the trend of power electronics has been shown in the four fields of source, network, load and storage [1-3]. In terms of transmission system, voltage source converter based multi-terminal direct current (VSC-MTDC) system is suitable for grid connection and consumption of large-scale renewable energy, and has been widely used [4-5]. Inter-station coordination control of VSC-stations is one of the key controls for stable operation of the VSC-MTDC system. The current inter-station coordination control methods of the VSC-MTDC system are mainly master-slave control, voltage margin control and droop control. Among them, droop control is currently the most applied method of inter-station coordination control by virtue of the advantage of cooperative imbalance power dissipation by multiple stations [6]. However, the essence of droop control is to change the DC voltage to achieve tidal redistribution to dissipate the unbalanced power, and the deviation of DC voltage will affect the normal operation of the system.

The problem of DC voltage deviation inherent in the use of droop control to dissipate unbalanced power in VSC-stations has been extensively studied by scholars. In [7], the error input in the proportional form is changed to the proportional-integral (PI) form by using a Washout filter instead of a droop coefficient to eliminate the control static difference and achieve DC voltage stabilization control. In [8], the DC voltage deviation is superimposed on the droop control, and the zero-error adjustment of the DC voltage is realized by using the zero-error characteristics of the PI controller. However, this control method transforms the droop control station into a DC voltage control station and loses the ability of the droop control station to coordinate the unbalanced power dissipation of multiple stations. Ref. [9-11] proposes an adaptively adjusted droop control method, which achieves a reasonable distribution of unbalanced power and suppresses the dynamic deviation of the DC voltage by adjusting the droop coefficient. In [12-13], the unbalanced power of the system is superimposed on the active power loop in the droop control, and the VSC-station is operated near the DC voltage rating by moving the droop curve. Ref. [14] proposes to calculate the system unbalanced power by DC voltage deviation and then adjust the droop control active power reference value. However, this method is sensitive to the droop coefficient and DC voltage, and the amount of power deviation needs to be obtained indirectly from the DC voltage deviation.

Aiming at the problem of DC voltage deviation in droop control, this paper proposes an optimized droop control with DC voltage dynamic correction. The main contributions are as follows:

(1) Through theoretical analysis, this paper demonstrates that when the VSC-station with droop control dissipates the unbalanced power to reach the steady state, it is impossible to restore the DC voltage to the initial state with constant power.

(2) By introducing the power margin and DC voltage of the VSC-station into the droop coefficient, it ensures that the droop VSC-station with smaller power margin bears less unbalanced power, and the droop control station with larger power margin bears more unbalanced power, which optimizes the tidal current distribution of the system and reduces the DC voltage deviation.

(3) Aiming at the problem that the optimal droop control can only adjust the DC voltage after the stability of the VSC-station, a DC voltage stabilizer is designed. The DC voltage variation is used as the input to simulate the inertia response of the synchronous generator, and the active power reference value is automatically adjusted during the power disturbance process to restore the DC voltage.

Finally, the simulation results in PSCAD/EMTDC verify the effectiveness of the proposed coordinated control strategy. The rest of the paper is organized as follows. Section 2 briefly describes the basic structure of VSC-MTDC systems and the working principle of the conventional droop controller. Section 3 proves by mathematical derivation that it is infeasible to restore the DC voltage to the initial state when the output active power of the VSC-station keeps constant after the system is

disturbed. On this basis, an adaptive droop control strategy considering the VSC-station real-time power margin is proposed to restore the DC voltage to the state closest to the initial value. The presented approach is verified on PSCAD/EMTDC in Section 4. The conclusions of this paper are outlined in Section 5.

2 MTDC SYSTEM STRUCTURE AND CONTROL

The structure diagram of the parallel type five-terminal VSC-MTDC systems is shown in Fig. 1. The DC sides of the five VSC-stations are connected in parallel through the DC network. The active power transmitted by each VSC-station in this system is injected into the AC grid as the reference positive direction.

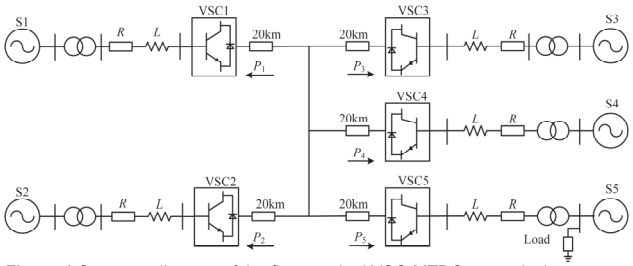

Figure 1 Structure diagram of the five-terminal VSC-MTDC transmission system

2.1 Converter Modeling

The physical structure of VSC is shown in Fig. 2, in a two-phase rotating coordinate system, the mathematical model of VSC may be stated as follows.

$$\begin{cases} L\dfrac{\mathrm{d}i_{\mathrm{sd}}}{dt}+Ri_{\mathrm{sd}}=U_{\mathrm{sd}}-U_{\mathrm{d}}+\omega Li_{\mathrm{sq}} \\ L\dfrac{\mathrm{d}i_{\mathrm{sq}}}{dt}+Ri_{\mathrm{sq}}=U_{\mathrm{sq}}-U_{\mathrm{q}}-\omega Li_{\mathrm{sd}} \end{cases} \tag{1}$$

where i_{sd} and i_{sq} represent the d and q components of the current flowing from the AC system to the converter side. U_{sd} and U_{sq} represent the d and q components of the VSC output AC voltage. U_{d} and U_{q} represent the d and q components of the AC voltage at the point of common coupling. ω represents the angular frequency of the AC system [15].

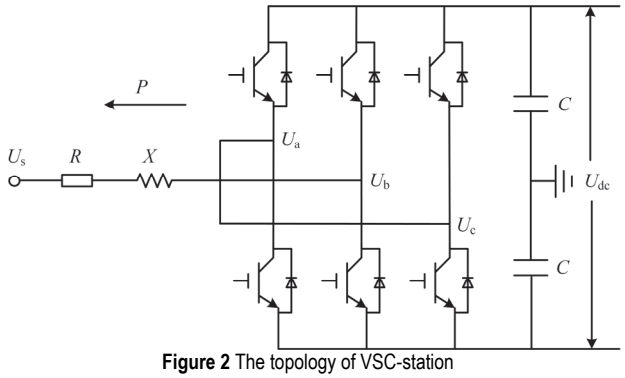

Figure 2 The topology of VSC-station

The overall control structure of the system includes the outer loop control and the inner loop control. The outer loop controller contains two types of control: active power control and reactive power control, and the tracking of the control quantity to the reference value is realized. The inner loop control mainly tracks the current reference value output by the outer loop and converts it into a voltage signal to generate a PWM pulse, thereby controlling the on-off of the device in the VSC-station [16-17]. The double-loop control structure of VSC-MTDC is shown in Fig. 3.

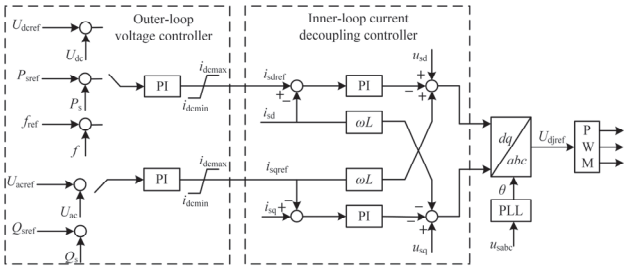

Figure 3 Dual-loop control block diagram of VSC-MTDC systems

2.2 Analysis of the Droop Control Characteristics

The droop control stabilizes the DC voltage through multiple VSC-stations with power regulation capabilities. The structure of the DC voltage droop controller is shown in Fig. 4. P_{sref} and P_{s} represent the active power command value and measured value. U_{dcref} and U_{dc} represent the DC voltage command value and measured value. k is the droop coefficient and PI is the proportional-integral controller [18-19].

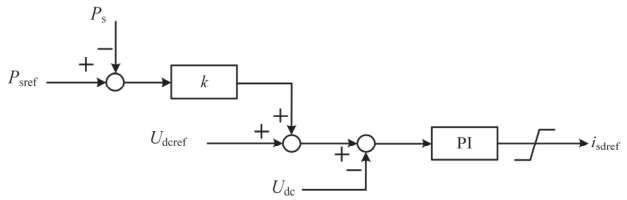

Figure 4 DC voltage droop controller

In Fig. 4, the following is the relationship between active power and DC voltage.

$$P_{\mathrm{sref}}-P_{\mathrm{s}}+\frac{U_{\mathrm{dcref}}-U_{\mathrm{dc}}}{k}=0 \tag{2}$$

It is assumed that there are NVSC-stations in the VSC-MTDC systems with droop control strategy, the i ($1 \le i \le N$) VSC-station's unbalanced power ΔP_i and the DC voltage variation ΔU_{dc} have the following relationship.

$$\Delta P_i=-\frac{\Delta U_{\mathrm{dc}}}{k_i} \tag{3}$$

To ensure the power balance of the DC network, the sum of the active power shared by each VSC-station should be equal to the power disturbance value ΔP in the DC network.

$$\Delta P=\sum_{i=1}^{N}\Delta P_i=-\Delta U_{\mathrm{dc}}\sum_{i=1}^{N}\frac{1}{k_i} \tag{4}$$

Combing Eq. (3) and Eq. (4), we get:

$$\Delta P_i = \frac{\Delta P}{k_i \sum_{i=1}^{N} \frac{1}{k_i}} \tag{5}$$

It can be seen from Eq. (5) that when each VSC-station's droop coefficient is fixed, the unbalanced power assumed by the VSC-station during the adjustment process is inversely proportional to its droop coefficient. That is to say, the larger the droop coefficient of the VSC-station, the smaller unbalanced power it bears. When the system is disturbed, the DC voltage is bound to have deviations due to unbalanced active power distribution. This provides a research direction for adaptive droop control based on DC voltage deviation-free correction in Section 3.

3 MTDC SYSTEM STRUCTURE AND CONTROL

The degree of active power and DC voltage departure from the rated value at the VSC-station is an essential measure of stability for VSC-MTDC systems. When using the conventional droop control method, as the measured power approaches the reference power, the gap between the measured DC voltage and the reference DC voltage should decrease [20].

3.1 DC Voltage Deviation-free Correction Feasibility Analysis

In the VSC-MTDC systems, the output active power of the VSC-station can also be expressed as:

$$P_{i1} = \sum_{i \neq j} \frac{U_{\mathrm{dc}i1}(U_{\mathrm{dc}i1} - U_{\mathrm{dc}j1})}{R_{ij}} \tag{6}$$

where R_{ij} is the line resistance between the VSC-stations, $1 \leq i \leq N$, $1 \leq j \leq N$. $U_{\mathrm{dc}j1}$ is the initial DC voltage of VSC$_j$ connected to VSC$_i$.

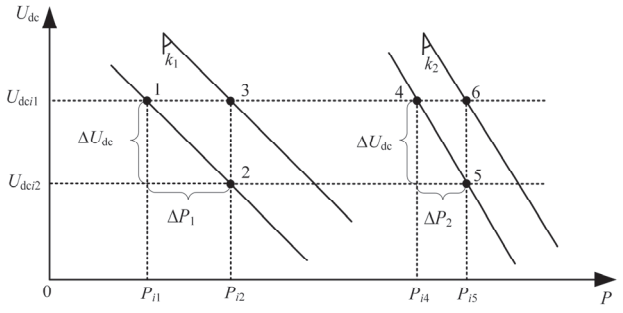

Figure 5 Droop control operating point change

As shown in Fig. 5, we can obtain.

$$\begin{cases} P_{i2} = P_{i1} + \Delta P_1 \\ P_{i2} = P_{i3} \end{cases} \tag{7}$$

$$\begin{cases} U_{\mathrm{dc}i1} = U_{\mathrm{dc}i2} + \Delta U_{\mathrm{dc}} \\ U_{\mathrm{dc}i1} = U_{\mathrm{dc}i3} \\ \Delta U_{\mathrm{dc}} = -k_1 \times \Delta P_1 \end{cases} \tag{8}$$

Combing Eq. (6) and Eq. (7), we get:

$$\sum_{i \neq j} \frac{U_{\mathrm{dc}i1}(U_{\mathrm{dc}i1} - U_{\mathrm{dc}j1})}{R_{ij}} + \Delta P_1 = \sum_{i \neq j} \frac{U_{\mathrm{dc}i3}(U_{\mathrm{dc}i3} - U_{\mathrm{dc}j3})}{R_{ij}} \tag{9}$$

Combing Eq. (8) and Eq. (9), we get:

$$\Delta P_1 = -\frac{\Delta U_{\mathrm{dc}}}{k_1} = 0 \tag{10}$$

From Eq. (10), ΔP_1 is equal to 0, and as known from Fig. 5, ΔP_1 is not equal to 0 due to the existence of unbalanced power. Therefore, it is impossible to realize the DC voltage deviation-free correction under the condition that the output power of the VSC-station remains constant. On the contrary, at the expense of the change of the output power of the VSC-station, the DC voltage can be restored to a state close to the initial value, and the "difference-free" regulation of the DC voltage can be achieved approximately [21-22].

3.2 Optimal Adaptive Droop Coefficient Optimization Strategy

Section 3.1 proves that deviation-free correction of DC voltages without power variations is impossible. The control strategy in this paper is as follows, which can approximate the deviation-free correction of DC voltage based on the rational allocation of unbalanced power. Define the available real-time power margin of the VSC-station as P_{can}, and the DC voltage variation as U_{can}, which can be expressed as:

$$P_{\mathrm{can}} = \begin{cases} P_{\max} - P_{\mathrm{s}} & \Delta U_{\mathrm{dc}} < 0 \\ P_{\max} + P_{\mathrm{s}} & \Delta U_{\mathrm{dc}} > 0 \end{cases} \tag{11}$$

$$U_{\mathrm{can}} = \begin{cases} U_{\mathrm{dcmax}} - U_{\mathrm{dcref}} & \Delta U_{\mathrm{dc}} > 0 \\ U_{\mathrm{dcref}} - U_{\mathrm{dcmin}} & \Delta U_{\mathrm{dc}} < 0 \end{cases} \tag{12}$$

where $P_{\max}$ represents the maximum power allowed to be transmitted by the VSC-station. U_{dcmax} and U_{dcmin} represent the maximum and the minimum value of DC voltage allowed by the system.

The droop coefficient for optimal adaptive adjustment can be expressed as:

$$k_i = \frac{\alpha \times U_{\mathrm{can}}}{P_{\mathrm{can}}} \tag{13}$$

where α represents the voltage deviation factor, which is to keep the DC voltage fluctuation within the allowable range of the system. α can be expressed as:

$$\alpha = 0.5 + 0.5 \frac{\Delta U_{\mathrm{dc}}}{U_{\mathrm{can}}} \mathrm{sgn}(\Delta U_{\mathrm{dc}}) \tag{14}$$

When the deviation between the DC voltage measured value and commanded value is more minor, the voltage

deviation coefficient α is closer to 0.5, which is the same as decreasing the fraction of the adaptive droop control's DC voltage regulation. As the DC voltage deviation decreases, α increases accordingly, which provides a sufficient adjustment amount for the update of the droop coefficient when the system is in a transient state.

Substituting Eq. (13) into Eq. (5), we get:

$$\Delta P_i = \frac{\Delta P}{\sum_{i=1}^{N} P_{\mathrm{can}i}} P_{\mathrm{can}i} \tag{15}$$

It can be seen from Eq. (15) that the unbalanced power assumed by each VSC-station is determined by its real-time power margin. The larger the real-time power margin of the VSC-station, the larger the unbalanced power it bears, which effectively avoids the problem of overloading the VSC-station caused by the excessive unbalanced power of the system.

3.3 Droop Control Strategy with Additional DC Voltage Stabilizer

Aiming at the problem that the optimal droop control can only perform DC voltage regulation after the VSC-station is stabilized, a DC voltage stabilizer is designed to reduce the DC voltage deviation in the dynamic process. Analog to the inertia method of synchronous generator, take ΔU_{dc} as input, and reduce the DC voltage change value by adjusting the power reference value during power disturbance [23]. Taking Eq. (11), Eq. (12), Eq. (13), and Eq. (14) into consideration, the optimal adaptive droop control with an additional DC voltage stabilizer is depicted in Fig. 6.

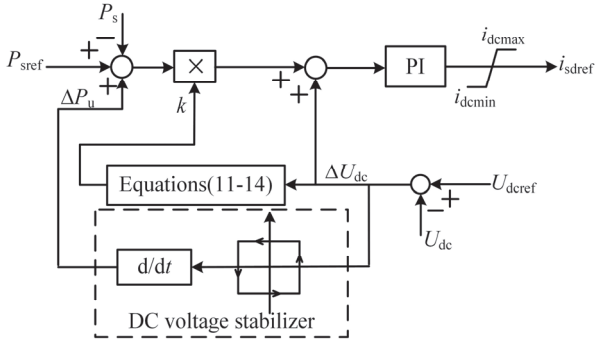

Figure 6 Block diagram of optimal adaptive droop control with additional DC voltage stabilizer

As shown in Fig. 6, to avoid frequent fluctuations in the system due to DC voltage fluctuations, a dead zone is added after ΔU_{dc}. At the moment of power disturbance, ΔU_{dc} is large enough to provide sufficient regulation for the update of the active power command value. At the end of the dynamic process, ΔU_{dc} is zero and no longer participates in regulation.

4 ANALYSIS OF SIMULATION RESULTS

To verify the effectiveness of the proposed control strategy, a five-terminal flexible DC system is built on the simulation software PSCAD/EMTDC platform as shown in Fig. 1.

Table 1 Main parameters of the VSC-MTDC systems

Parameters	Numerical value
Active power reference value / MW	200
DC voltage reference value / kV	400
Rated capacity of VSC1~VSC5 stations / MW	250/200/200/150/150
Active power command value of VSC1~VSC5 / MW	−220/−100/115/85/100
DC capacitance / μF	1000
Limit of the voltage deviation	±7.5%
Coupling transformer ratio	220/200

The comparative experimental control method used in this paper is as follows:
CM1: Conventional droop control.
CM2: The control method proposed in [19].
CM3: The control strategy proposed in this paper.

4.1 VSC3 Active Power Occurs inSteps

t = 5 s, the active power command value of VSC3 rises from 0.575 (p.u.) to 0.9 (p.u.), the comparative analysis of the simulation results under the three control strategies is shown in Fig. 7 and Tab. 2.

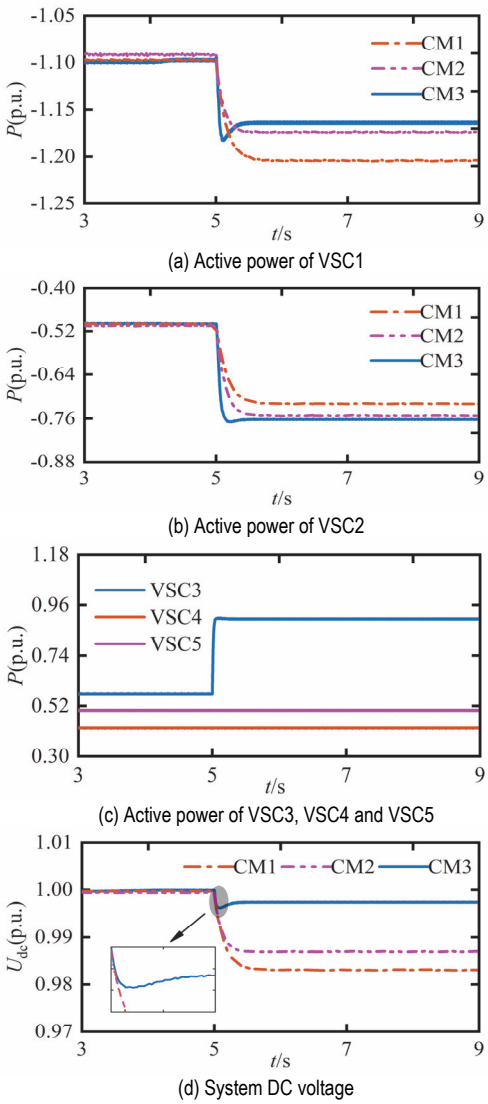

Figure 7 Simulation results of VSC3 power variation

As can be seen from Fig. 7, in the initial state, due to system losses, the actual power of VSC1 and VSC2 under the three control strategies is close to the power command value, but there is a slight difference. The DC voltage gradually decreases after the VSC3 power command value is changed. For CM1, VSC1 and VSC2 dissipate the unbalanced power according to a fixed ratio, and the transmitted power changes from −1.098 (p.u.) and −0.500 (p.u.) to −1.204 (p.u.) and −0.720 (p.u.), respectively, and the DC voltage decreases from 0.999 (p.u.) to 0.983 (p.u.). For CM2, the droop coefficient is calculated from a fixed power margin, and the system power distribution is optimized, the transmitted power varies from −1.092 (p.u.) and −0.506 (p.u.) to −1.174 (p.u.) and −0.750 (p.u.), respectively, and the DC voltage is reduced from 0.999 (p.u.) to 0.987 (p.u.).

For CM3, the droop coefficient is automatically adjusted according to the real-time power margin of the VSC-station to further optimize the system power distribution. The transmitted power changes from −1.098 (p.u.) and −0.498 (p.u.) to −1.162 (p.u.) and −0.763 (p.u.), respectively, and the DC voltage decreases from 0.999 (p.u.) to 0.997 (p.u.). As can be seen from Fig. 7d, the DC voltage deviation rates are 1.66%, 1.25% and 0.27% for the three control strategies, respectively. Compared with the other two control strategies, the DC voltage deviation under CM3 is the smallest, and an additional DC voltage stabilizer dynamically adjusts the power value, the system enters the DC voltage recovery state at t = 5.06 s.

Table 2 Simulation results of DC voltage deviation

Control strategy	CM1	CM2	CM3
Initial DC voltage / kV	399.88	399.78	399.97
Steady-state DC voltage / kV	393.25	394.79	398.88
DC voltage deviation / kV	6.63	4.52	1.09
DC voltage deviation rate / %	1.66	1.25	0.27

4.2 VSC4 Active Power Occurs in Steps

t = 4 s, the active power command value of VSC4 rises from 0.425 (p.u.) down to 0.075 (p.u.), the comparative analysis of the simulation results under the three control strategies is shown in Fig. 8 and Tab. 3.

The DC voltage gradually increases after the VSC4 power command value is changed. For CM1, the transmitted power varies from −1.097 (p.u.), −0.500 (p.u.) to -−0.985 (p.u.), −0.268 (p.u.) and the DC voltage increases from 0.999 (p.u.) to 1.017 (p.u.), respectively. For CM2, the droop coefficient is calculated from the fixed power margin of the VSC-station, the transmitted power varies from −1.092 (p.u.) and −0.504 (p.u.) to −0.874 (p.u.) and −0.375 (p.u.), respectively, and the DC voltage increases from 0.999 (p.u.) to 1.002 (p.u.).

For CM3, the droop coefficient is automatically adjusted by the real-time power margin of the VSC- station, and the power reference value is adjusted during the power disturbance to reduce the amount of DC voltage variation. The transmitted power changes from -1.098 (p.u.) and −0.499 (p.u.) to −0.917 (p.u.) and −0.334 (p.u.), respectively, and the DC voltage decreases from 0.9998 (p.u.) to 0.9993 (p.u.). From Fig. 8d, it can be seen that the DC voltage deviation rates are 1.75%, 0.49% and 0.21% for the three control strategies, respectively.

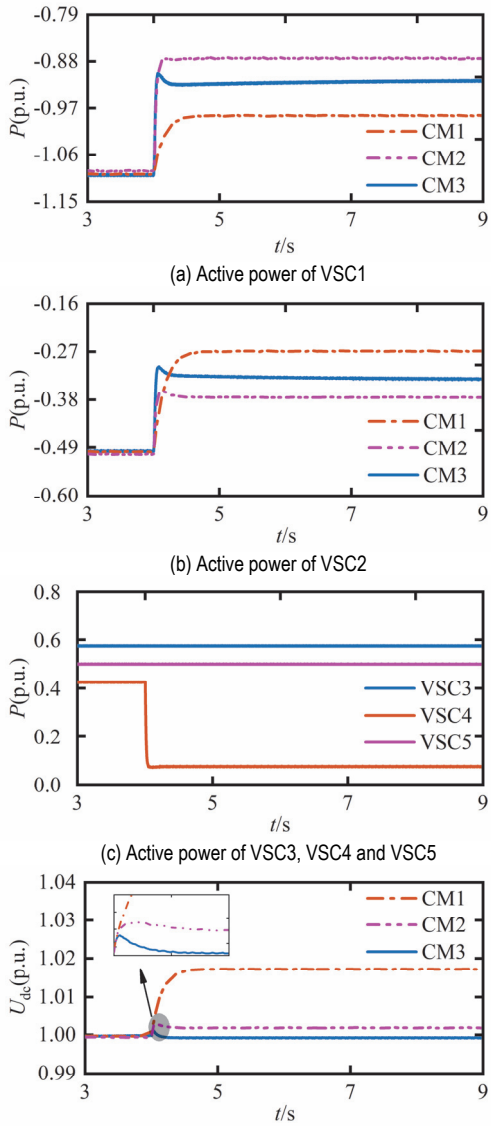

Figure 8 Simulation results of VSC4 power variation

According to the above analysis, when the system power fluctuates, the control strategy in this paper can reasonably distribute the unbalanced power according to the system status, reduce the DC voltage deviation, and improve the stability and reliability of the VSC-MTDC system operation.

Table 3 Simulation results of DC voltage deviation

Control strategy	CM1	CM2	CM3
Initial DC voltage / kV	399.88	399.76	399.89
Steady-state DC voltage / kV	406.87	401.74	400.72
DC voltage deviation / kV	6.99	1.98	0.83
DC voltage deviation rate / %	1.75	0.49	0.21

4.3 The VSC2 Exits when the System is Running Normally

VSC-MTDC system should satisfy the $N-1$ principle, any VSC-station in the system is out of operation, and the rest of the VSC-stations in the system should have the power regulation capability to stabilize the DC voltage. t = 3 s, the operation of the VSC2 exit, the comparative analysis of the simulation results under the three control strategies is shown in Fig. 9 and Tab. 4.

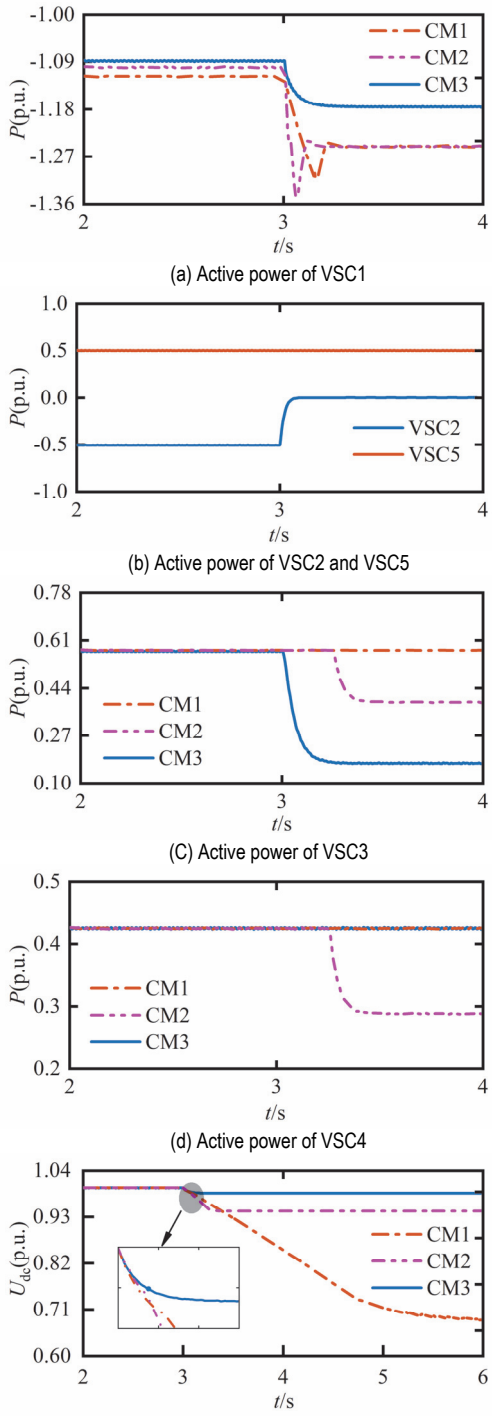

Figure 9 VSC2 exit operation simulation

From Fig. 9b, it can be seen that VSC1 and VSC2 jointly maintain the power balance of the DC network before the fault occurs. With VSC2 out of operation, its power transfer value drops to 0. The unbalanced power appearing in the DC network causes the DC voltage to drop rapidly. For CM1, VSC1, as the only power balancing point, undertakes the power balancing task of the system, and its delivered active power soon changes to −1.250 (p.u.), reaching full load and switching to constant power operation, losing the ability to control DC voltage. Eventually, the DC voltage continues to drop below the limit value of 0.925 (p.u.), and the whole DC system will become unstable and stop operating.

For CM2, when the DC voltage is not lower than 0.950 (p.u.), VSC1 acts as the only power balancing point and undertakes the power balancing task of the system, and its transmitted power changes to −1.250 (p.u.), switching to constant power operation and losing the ability to control the DC voltage. Since there is still some unbalanced power in the DC network causing a continuous decrease in DC voltage, VSC3 and VSC4 shift their control mode to take up the task of dissipating unbalanced power and stabilizing DC voltage. When the system reaches steady state, the DC voltage drops to 0.944 (p.u.).

For CM3, since the power margin of VSC1 is not sufficient to dissipate the unbalanced system power, VSC3 shifts control mode to cooperate with VSC1 to dissipate the unbalanced system power. When the system reaches steady state, VSC1 does not reach full load and still has the ability to stabilize the DC voltage. From Fig. 9e, it can be seen that the DC voltage deviation rates are 31.5%, 5.54% and 1.28% for the three control strategies, respectively.

Table 4 Simulation results of DC voltage deviation

Control strategy	CM1	CM2	CM3
Initial DC voltage / kV	399.85	399.89	399.79
Steady-state DC voltage / kV	273.88	377.75	394.68
DC voltage deviation / kV	125.97	22.14	5.11
DC voltage deviation rate / %	31.5	5.54	1.28

5 CONCLUSION

Droop control does not require inter-station communication, but its ability to control DC voltage and active power is fixed and difficult to adapt to various complex operating conditions. Therefore, this paper proposes a droop control optimization strategy to adjust the droop coefficient according to the power margin of the converter station in real time to optimize the system current distribution and reduce the DC voltage deviation. A five-terminal flexible DC transmission model is developed using PSCAD/EMTDC. Comparing the control strategy proposed in this paper with the other two strategies, the results demonstrate that the control strategy of this paper can effectively enhance the power distribution capability with minimum DC voltage deviation when power fluctuation occurs in the DC system. It is also verified that the control strategy can run stably in *N*-1 mode, which proves the reliability of the control strategy running in the system.

Acknowledgements

This work is jointly supported by the Scientific and Technological Research Foundation of Henan Province (No. 222102320198), and the Key Project of Zhengzhou University of Light Industry (No. 2020ZDPY0204), and the Smart Grid Sichuan Provincial Key Laboratory 2022 Open Fund Project (NO. 2022-IEPGKLSP-KFYB01).

6 REFERENCES

[1] Sun, K. Q., Xiao, H. Q., & Liu, Y. L. (2022). Optimized allocation method of the VSC-MTDC system for frequency regulation reserves considering ancillary service cost. CSEE *Journal of Power and Energy Systems*, *8*(1), 53-63. https://doi.org/10.17775/CSEEJPES.2020.05800

[2] Wang, J. & Lu, J. P. (2015). Fuzzy logic system for frequency stability analysis of wind farm integrated power systems. *Technical gazette*, *22*(5), 1199-1208. https://doi.org/10.17559/TV-20140708055807
[3] Mochamad, R. & Preece, R. (2019). Assessing the impact of VSC-HVDC on the interdependency of power system dynamic performance in uncertain mixed AC/DC systems. *IEEE Transactions on Power Systems*, *35*(1), 63-74. https://doi.org/10.1109/TPWRS.2019.2914318
[4] Li, B. H., Liu, T. Q., & Zhang, Y. M. (2017). Unified adaptive droop control design based on dynamic reactive power limiter in VSC-MTDC. *Electric Power Systems Research*, *148*, 18-26. https://doi.org/10.1016/j.epsr.2017.03.010
[5] Li, H., Meng, K., Li, X., & Peng, Y. F. (2022). Simulation of wind power integration with modular multilevel converter-based high voltage direct current. *Technical gazette*, *29*(1), 301-307. https://doi.org/10.17559/TV-20210729043234
[6] Liu, H. Y., Liu, C. R., Zheng, L., & Wang, Q. Q. (2022). Cooperative optimal droop control for VSC-MTDC system with quasi non-error DC voltage regulation. *Automation of Electric Power Systems*, *46*(6), 117-126.
[7] Wan, Q. Z., Li, J. T., & Chi, Z. J. (2019). Power smoothing control strategy for renewable energy based DC grid. *High Voltage Engineering*, *45*(1), 276-283.
[8] Yuan, Z. C., Wu, Z. L., Jin, Q., Jiang, S. G., & Huang, Y. (2018). Frequency stabilization control strategy with DC voltage secondary regulation of VSC-MTDC based interconnected systems. *Automation of Electric Power Systems*, *42*(23), 9-13.
[9] Liu, Y. P., Xie, S., Liang, H. P., & Xie, Q. (2020). Adaptive droop control strategy for VSC-MTDC system considering DC voltage errors among converter stations. *Transactions of China Electrotechnical Society*, *35*(15), 3270-3280.
[10] Wang, W. Y., Li. Y., Cao, Y. J., U, & Hager, C. R. (2018). Adaptive droop control of VSC-MTDC system for frequency support and power sharing. *IEEE Transactions on Power Systems*, *33*(2), 1264-1274. https://doi.org/10.1109/TPWRS.2017.2719002
[11] Wang, W. Y., Xin, Y., Cao, Y. J., Jiang, L., & Li, Y. (2021). A distributed cooperative control based on consensus protocol for VSC-MTDC Systems. *IEEE Transactions on Power Systems*, *36*(4), 2877-2890. https://doi.org/10.1109/TPWRS.2021.3051770
[12] Wu, G. H., Du, Z. C., Zhao, Y. Y., & Li, G. Y. (2021). Flexible controls to reduce DC voltage deviations in multi-terminal DC grids. *IET Generation, Transmission & Distribution*, *15*(12), 1830-1840. https://doi.org/10.1049/gtd2.12138
[13] Li, Z., Li, Y. Z., Lu, Y. P., Zhan, R. P., He, Y., & Zhang, X. P. (2019). Active power balance oriented coordinating control strategy for VSC-MTDC system. *Automation of Electric Power Systems*, *43*(17), 117-124.
[14] Xu, Z., Zhang, Z. R., & Liu, G. R. (2017). Research on voltage control principle of flexible DC transmission power grid. *Electric Power Engineering Technology*, *36*(1), 54-59.
[15] Ke, L. Z., Liu, Z. X., & Zhang, Y. (2020). Diagnosis and location of open-circuit fault in modular multilevel converters based on high-order harmonic analysis. *Technical gazette*, *27*(3), 898-905. https://doi.org/10.17559/TV-20190904105201
[16] Li, Y. Y., Liu, K. P., Zhu, S., Huai, Q., & Liao, X. B. (2021). DC side impedance modelling and stability analysis of VSC-MTDC system. *High Voltage Engineering*, *47*(8), 627-638.
[17] Li, M. H., Liu, X. M., & Chen, P. (2016). Fast voltage margin control strategy for VSC-MTDC systems. *Power System Technology*, *40*(10), 3045-3051.
[18] Li, Z., Zhang, T. Q., Wang, Y. R., Tang, Y., & Zhang, X. P. (2022). Fault Self-Recovering Control Strategy of Bipolar VSC-MTDC for Large-Scale Renewable Energy Integration. *IEEE Transactions on Power Systems*, *37*(4), 3036-3047. https://doi.org/10.1109/TPWRS.2021.3127192
[19] Zhu, R. K., Li, X. Y., & Wu, F. (2015). A novel droop control strategy taking into account the available headroom for VSC-MTDC system. *Journal of Sichuan University*, *47*(3), 137-143.
[20] Liu, Y. C., Wu, J., Liu, H. Y., & Xu, D. G. (2016). Effective power sharing based on adaptive droop control method in VSC multi-terminal DC Grids. *Proceedings of the CSEE*, *36*(1), 40-48.
[21] Mi, G. S., Kan, J., Gao, L., Deng, Y., & Zhao, Y. (2020). Optimized droop control strategy for voltage sourced converterbased multi-terminal HVDC. *Proceedings of the CSU-EPSA*, *32*(1), 101-107.
[22] Zhao, X. D. & Li, K. (2015). Droop setting design for multi-terminal HVDC grids considering voltage deviation impacts. *Electric Power Systems Research*, *123*, 67-75. https://doi.org/10.1016/j.epsr.2015.01.022
[23] Sun, L. X., Chen, Y., Song, H. G., Cao, H., & Wang, Q. (2016). Improved Voltage Droop Control Strategy for VSC-MTDC. *Power System Technology*, *40*(4), 1037-1043.

Contact information:

Ping HE, professor
(Corresponding author)
School of Electrical and Information Engineering,
Zhengzhou University of Light Industry, 450002, China
E-mail: hplkz@126.com

Xiaowei ZHANG
School of Electrical and Information Engineering,
Zhengzhou University of Light Industry, 450002, China
E-mail: 1458696052@qq.com

Congshan LI, professor
School of Electrical and Information Engineering,
Zhengzhou University of Light Industry, 450002, China
E-mail: 543627767@qq.com

Lei YUN
School of Electrical and Information Engineering,
Zhengzhou University of Light Industry, 450002, China
E-mail: 642183255@qq.com

Hua YANG
School of Electrical and Information Engineering,
Zhengzhou University of Light Industry, 450002, China
E-mail: 871454827@qq.com

Yabang YAN
School of Electrical and Information Engineering,
Zhengzhou University of Light Industry, 450002, China
E-mail:2572702342@qq.com